

THERMAL CHARACTERIZATION OF WARIFTEINE BY MEANS OF TG AND A DSC PHOTOVISUAL SYSTEM

*C. F. S. Aragão, J. M. B. Filho and R. O. Macêdo**

Laboratório de Tecnologia Farmacêutica, UFPB, Campus I, João Pessoa, Paraíba, CEP 59059-900
Brasil

Abstract

This work proposes thermal characterization as analytical methodology for the identification and purity assay of warifteine, an alkaloid in *Cissampelos sympodialis* Eichl. Thermal and kinetic parameters were determined by means of TG and DSC photovisual studies. The TG results showed that the decomposition of warifteine in air and nitrogen atmospheres proceeds in three and four steps, respectively. The TG data allowed calculation of the kinetic parameters of warifteine. The activation energy values obtained by different methods displayed a good correlation. With the DSC photovisual system applied it is possible to detect the impurity level in warifteine after its purification.

Keywords: DSC photovisual, TG, warifteine

Introduction

An important contribution to the chemistry of natural products has been made by investigations of medicinal plants used traditionally in therapy. Heat can give rise to alterations in the chemical composition in that plant part being studied [1].

The DSC photovisual system is currently being introduced as a thermal analytical method which combines microscopic imaging and DSC data. The thermal properties of substances are of interest in different quality control areas, and the various techniques (TG, DSC, DTA and TMA) have become powerful analytical tools [2, 3].

Thermal behaviour studies in which thermal techniques are applied to naturally occurring substances are rather scarce in the literature. The present work deals with a characterization of warifteine by means of TG and DSC photovisual data.

Experimental

Warifteine was obtained from powdered leaves of *Cissampelos sympodialis* (Menispermaceae): a 95% hydroalcoholic extract obtained by maceration was submitted to

* Author for correspondence: E-mail: ruimacedo@ltf.ufpb.br; Fax: 55-83-216-7371

separation techniques to isolate the alkaloids. The warifteine was purified and identified by means of its ^1H and ^{13}C NMR spectral data, which were in agreement with literature [4].

The TG curves were obtained with a Shimadzu thermobalance, model TG-50H, under a synthetic air flow of 20 ml min^{-1} or a N_2 flow of 50 ml min^{-1} , at heating rates of 5, 10, 15 and $20^\circ\text{C min}^{-1}$ up to 900°C . A sample mass of about 5 mg was packed in an alumina cell.

As concerns DSC coupled to the photovisual system, data were obtained with a Shimadzu differential scanning calorimeter (model DSC-50), an Olympus microscope connected to a high-resolution camera (model VCC-D520, Sanyo) and image capture software. Samples were heated in an aluminium pan, in the temperature interval $25\text{--}500^\circ\text{C}$, at heating rates of 5, 10 and $15^\circ\text{C min}^{-1}$. The nitrogen flow rate was 50 ml min^{-1} . The sample mass was 2.00 mg. The TG and DSC curves were analysed with TASYs software from Shimadzu. The DSC apparatus was calibrated via the melting points of indium ($156.6\pm 0.2^\circ\text{C}$) and zinc ($419.5\pm 0.3^\circ\text{C}$) standards. The heat flow and enthalpy were calibrated via the heat of fusion of indium ($28.58\pm 0.3\text{ J g}^{-1}$), under the same conditions as for the samples.

For the decomposition, the activation energy (E_a), the order of reaction (n) and the frequency factor (Z) were obtained from the first step of the TG curves. The kinetic parameters were calculated with α values of 0.1–0.9 by utilizing the mathematical equations of Coats–Redfern (CR) (Eqs (1) and (2)) [5], Madhusudanan *et al.* (MD) (Eqs (3) and (4)) [6], Horowitz–Metzger (HM) (Eqs (5) and (6)) [7], Van Krevelen (VK) (Eqs (7) and (8)) [8] and Ozawa (OZ) (Eq. (9)). The OZ parameters were obtained with TG curves recorded at a different heating rate.

The Coats–Redfern equations:

$$\text{For } n=1: \quad \log\left[\frac{-\ln(1-\alpha)}{T^2}\right] = \log\frac{AR}{\phi E} - \frac{E}{2303RT} \quad (1)$$

$$\text{For } n\neq 1: \quad \log\left[\frac{1-(1-\alpha)^{1-n}}{T^2(1-n)}\right] = \log\frac{AR}{\phi E} - \frac{E}{2303RT} \quad (2)$$

The equations of Madhusudanan et al.

$$\text{For } n=1: \quad \ln\left[\frac{-\ln(1-\alpha)}{T^{1.9206}}\right] = \ln\frac{AR}{\phi R} + 0.02 - 19206\ln\frac{E}{R} - 0.12040\frac{E}{RT} \quad (3)$$

$$\text{For } n\neq 1: \quad \ln\left[\frac{1-(1-\alpha)^{1-n}}{T^{1.9206}(1-n)}\right] = \ln\frac{AR}{\phi R} + 3.7678 - 19206\ln\frac{E}{R} - 0.1204\frac{E}{RT} \quad (4)$$

The Horowitz–Metzger equations:

$$\text{For } n=1: \quad \ln[-\ln(1-\alpha)] = \frac{E\theta}{RT_s} \quad (5)$$

$$\text{For } n \neq 1: \quad \ln\left[\frac{1-(1-\alpha)^{1-n}}{1-n}\right] = \frac{E\theta}{RT_s} \quad (6)$$

The Van Krevelen equations:

$$\text{For } n=1: \quad \log[-\ln(1-\alpha)] = \log\left[\frac{A\left(\frac{0.368}{T_s}\right)^{\frac{E}{RT_s}}}{\phi\left(\frac{E}{RT_s}+1\right)}\right] + (ERT_s+1)\log T \quad (7)$$

$$\text{For } n \neq 1: \quad \log\left[\frac{1-(1-\alpha)^{1-n}}{1-n}\right] = \log\left[\frac{A\left(\frac{0.368}{T_s}\right)^{\frac{E}{RT_s}}}{\phi\left(\frac{E}{RT_s}+1\right)}\right] + (ERT_s+1)\log T \quad (8)$$

The Ozawa equation:

$$\log\phi = \log\left[\frac{AE}{R_g(\alpha)}\right] - 2.315 - 0.4567\frac{E}{RT} \quad (9)$$

where α =fraction decomposed, T =temperature, A =frequency factor, R =gas constant, E =activation energy, ϕ =heating rate, and T_s =temperature of the peak.

Results and discussion

Thermogravimetric study

The TG curves of warifteine in air and N₂ atmospheres reveal three and four thermal decomposition stages, respectively, with temperature intervals depending on the heating rate. Table 1 presents the TG data relating to the temperature interval and mass loss for each step. The decomposition of warifteine was faster in air atmosphere than in nitrogen. Further, the mass losses in air (96.98%) and nitrogen (56.36%) were appreciably different. In air, the processes of thermal decomposition involved combustion. In nitrogen, warifteine underwent partial carbonization.

The kinetic data were calculated with five mathematical models. Table 2 presents the values of the order of reaction (n), the activation energy (E_a) and the frequency factor (Z) for warifteine, together with the best linear correlation coefficients

(*r*). It was found that the integral methods (Coats–Redfern and Madhusudanan *et al.*) and the approximation methods (Horowitz–Metzger and Van Krevelen) yielded kinetic data that were reasonably comparable with each other. However, the Ozawa method furnished data that differed from those obtained with the other methods.

Table 1 Thermogravimetric characteristics of warifteine in different atmospheres at a heating rate of 10°C min⁻¹

Atmosphere	Temperature interval/°C	Mass loss/%*
Air	265.7–371.5	12.50 (±0.27)
	371.5–576.5	24.57 (±0.22)
	576.5–771.7	59.91 (±0.24)
Nitrogen	270.1–349.4	17.68 (±0.18)
	349.4–418.8	16.88 (±0.20)
	418.8–723.7	13.94 (±0.16)
	723.7–898.2	7.86 (±0.20)

**n*=3

Table 2 Warifteine kinetic parameters obtained with the Coats–Redfern (CR), Madhusudanan *et al.* (MD), Ozawa (OZ), Horowitz–Metzger (HM) and Van Krevelen (VK) methods

Methods*	Kinetic parameters**		
	<i>n</i>	<i>E_a</i> /kJ mol ⁻¹	<i>Z</i> /s ⁻¹
CR	1.93 (±0.06)	110.14 (±0.75)	5.01 (±0.15)·10 ⁷
MD	1.84 (±0.04)	106.87 (±0.70)	2.61 (±0.10)·10 ⁷
HM	2.05 (±0.07)	121.30 (±0.80)	7.44 ((±0.20)·10 ⁸
VK	1.92 (±0.06)	112.29 (±0.75)	2.70 ((±0.10)·10 ¹³
OZ	0.60 (±0.03)	115.79 (±0.77)	8.42 (±0.22)·10 ⁹

* $\alpha=0.1-0.9$. For CR, $r=0.9905$; for MD, $r=0.9906$; for HM, $r=0.9916$; and for VK, $r=0.9884$ ***n*=3

The kinetic data, and especially the activation energy, were obtained for the characterization of warifteine, with a view to their future use as concerns the warifteine content in different dry extracts of *Cissampelos sympodialis*.

Calorimetric study

The DSC of warifteine, at a heating rate of 10°C min⁻¹, presented three peaks relating to phase transitions (Fig. 1). The first, at 252°C, is endothermic. The second peak, at 262.4°C, corresponds to an exothermic process. At this temperature, there is no mass loss (Fig. 1, curves 1 and 3), which indicates that this phase transition is related with a change in form of the warifteine molecule or the presence of another product. The third peak, at 352.2°C, is endothermic and accompanies a mass loss. At temperatures below 270°C, the DSC curve also exhibits the presence of shoulders, probably indicating other decomposition processes.

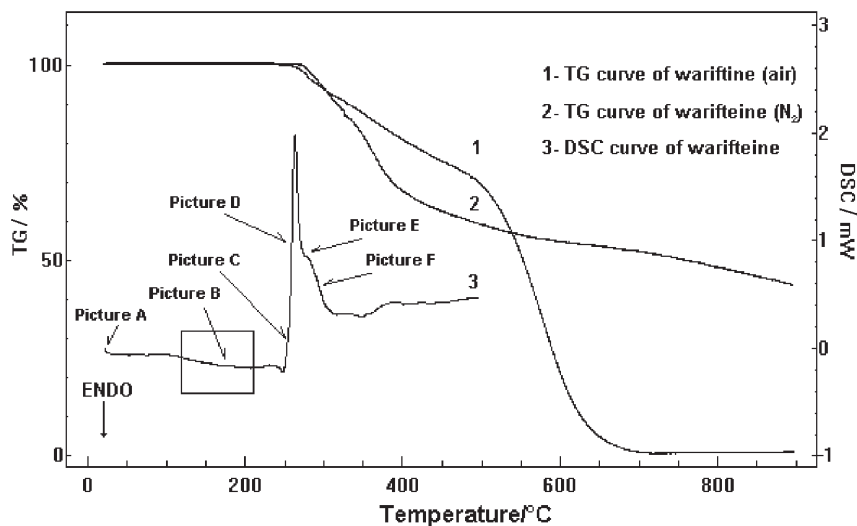


Fig. 1 TG and DSC curves of warifteine

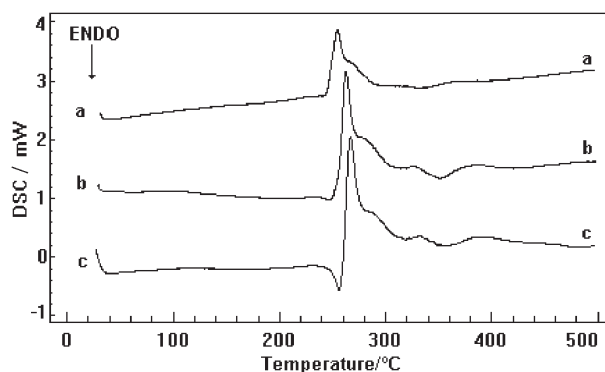


Fig. 2 DSC curves of warifteine at different heating rates, a – $5^{\circ}\text{C min}^{-1}$, b – $10^{\circ}\text{C min}^{-1}$, c – $15^{\circ}\text{C min}^{-1}$

The DSC curves in Fig. 2 reveal endothermic peaks at heating rates of 10 and $15^{\circ}\text{C min}^{-1}$ which are not observed at a heating rate of $5^{\circ}\text{C min}^{-1}$. The onset temperatures extrapolated for the exothermic peaks at heating rates of 5, 10 and $15^{\circ}\text{C min}^{-1}$ were 246, 256 and 259°C , respectively. The displacement of about 13°C between the heating rates of 5 and $15^{\circ}\text{C min}^{-1}$ could be explained by the heat capacity changes.

The pictures from the photovisual system (Fig. 3) demonstrated changes in colour in warifteine. This is verified in picture **A**, which shows the presence of two different crystals with different colours. The main compound, corresponding to most of the crystals, was yellow, while the secondary product was dark-orange. Picture **B**, at 182°C , depicts the melting point of the dark-orange crystals. Pictures **C** and **D**, at 254 and 257°C , exhibit dark substances (warifteine and impurity), with energetic trans-

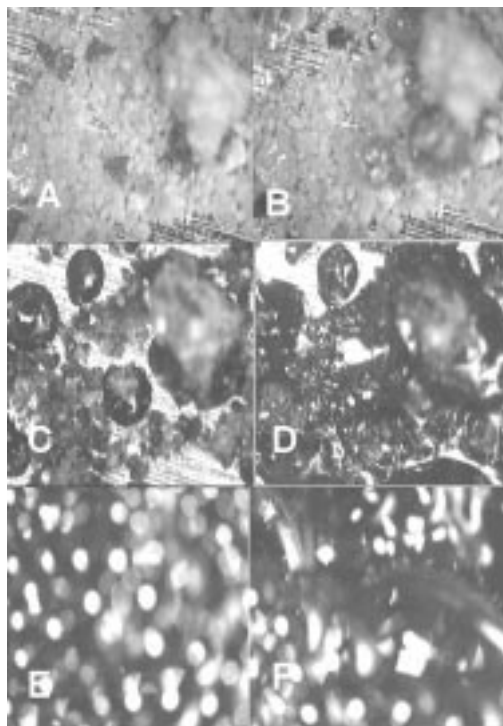


Fig. 3 Images of DSC photovisual system from warifteine. Images were taken at A – 25, B – 182, C – 254, D – 257, E – 280 and F – 290°C

formations in the molecule. Pictures **E** and **F** indicate the initial decomposition of the warifteine and impurity with photon emission visualization, followed by decomposition with mass loss. The photovisual system allowed visualization of a physico-chemical change (melting point) due to the impurity present in the warifteine in only small amount (approximately 1:100 (mass : mass) (Fig. 1, curves 3 – square in detail, and Fig. 3, Picture **B**).

The impurity detected as dark-orange crystals revealed a melting point at 182°C. Picture **B** could relate to dimethylwarifteine, with melting point between 188 and 190°C according to the literature [4].

Conclusions

The DSC photovisual technique allows the detection of the presence of impurity in warifteine that has been previously purified, this impurity not being detected by conventional DSC.

* * *

The authors thank ANVISA/MS and CNPq for financial support.

Reference

- 1 R. O. Macêdo, An. Assoc. Bras. Quim., 47 (1998) 313.
- 2 R. O. Macêdo, J. Therm. Anal. Cal., 56 (1999) 1323.
- 3 R. O. Macêdo, J. Therm. Anal. Cal., 59 (2000) 657.
- 4 J. L. Alencar, Novos alcalóides da *Cissampelos sympodialis* Eichl. MSc. Dissertation – UFPB/LTF, Paraíba, Brasil 1994.
- 5 A. W. Coats and J. P. Redfern, Nature, 201 (1964) 68.
- 6 P. M. Madhusudanan, K. Krishnan and K. N. Ninan, Thermochim. Acta, 221 (1993) 13.
- 7 H. H. Horowitz and R. Metzger, Anal. Chem., 35 (1963).
- 8 W. Van Krevelen, C. Van Heerden and F. Hutjens, Fuel, 30 (1951) 253.
- 9 T. Ozawa, Bull. Chem. Soc. Japan, 38 (1965) 1881.